On the Stability of Symmetric Quadrupedal Bounding Gaits via Factored Poincaré Maps

Xin Liu, and Ioannis Poulakakis

***Abstract*— Reduced-order models with springy massless legs have been employed extensively in the study of legged locomotion. Due to their hybrid nonlinear dynamics, analysis of such systems is often carried out numerically. In contrast, this paper adopts an analytical approach to study conditions for stability in a sagittal-plane model of quadrupedal bounding. Exploiting time-reversal symmetries possessed by the underlying vector fields, the corresponding Poincaré map can be factored in a way that allows the analytical formulation of conditions that are necessary for stability (and sufficient for instability) for bounding gaits. The method is then applied to facilitate the design of a leg recirculation controller for bounding gaits.**

I. Introduction

The method of Poincaré is often used to assess the existence and stability properties of periodic locomotion gaits [1]. However, the nonintegrability of the continuous-time vector fields precludes the analytical derivation of the Poincaré map and its linearization, thus hindering analytically tractable approaches. To seek insight more systematic than what numerical approaches provide, this paper concentrates on certain families of periodic running orbits – namely, those admitting time-reversal symmetries – and it formulates analytical conditions that are necessary for stability of a class of symmetric bounding motions.

Symmetry has played a key role in the development of controllers for running robots [2]. While symmetric motions can account for the coupling between the body and legs at steady state, asymmetry in the motion can generate stabilizing forces or can be used to accelerate and decelerate the system as in Raibert's three-part controller [3]. An analytical framework for studying stability of periodic locomotion gaits that exhibit certain symmetry characteristics has been introduced in [4]. In that work, a class of symmetry transformations – termed *time-reversal symmetries* [5] – is used to decompose the Poincaré map associated with symmetric hopping motions of the Spring Loaded Inverted Pendulum (SLIP) [6] in a way that allows the derivation of closed-form conditions that are necessary for stability. The method was subsequently used in [7] to investigate stability of a suitably controlled model of the hexapedal robot RHex.

At the core of the symmetry-based analytical methods discussed above are point-mass models like the SLIP [4], [6] and its extensions [7]. Such models however cannot capture the leg-torso coordination dynamics distributed over multiple stance and flight phases, which is a distinguished feature of bounding gaits [8]. Restricting attention to simplified models, much of the relevant literature on the analysis of bounding relies primarily on numerical studies of Poincaré maps [8]–[10]. Similarly, controllers for bounding – including diverse approaches based, for example, on delayed feedback control [11], [12], on central pattern generators [13], or on optimally-scaled hip force planning [14] – are developed without the aid afforded by analytical tools, such as those available for monopedal hoppers.

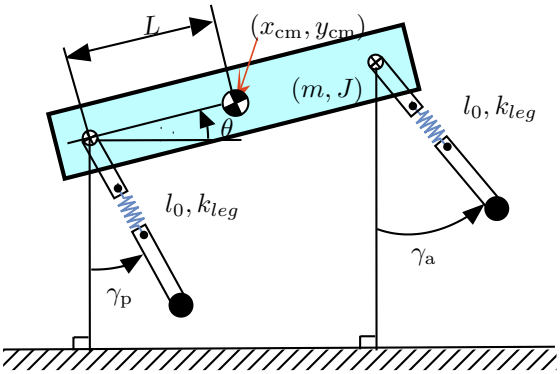

Fig. 1. A sagittal-plane bounding model with massless legs.

This paper develops an analytical framework for deriving conditions for stability of bounding gaits and applies it to ease controller design. The method introduced in [4] is adopted to study a sagittal-plane bounding model developed in a template setting; see Fig. 1. It is shown that the Poincaré map associated with the bounding gaits of interest can be factored in a way that allows the analytical computation of the (local) volume associated with the flow in a neighborhood of a fixed point. By requiring that the volume "shrinks" as the system evolves, a necessary condition for stable bounding can be analytically derived. The proposed method is then used to ease the design of a bounding controller.

II. Modeling Quadrupedal Bounding

In this work, the reduced-order model of Fig. 1 is employed to study quadrupedal bounding. The back and front virtual legs are assumed to be massless springs, representing the collective effect of the back and front physical leg pairs. The geometric and inertia parameters are given in Table I and they roughly correspond to the quadrupedal robot Scout II [8]. Figure 2 describes the footfall pattern of a nominal bounding gait; in this paper, we restrict our attention to bounding without double stance phase. Depending on whether a leg is on the ground or in flight, three different phases are distinguished; namely, the stance-anterior "sa",

X. Liu and I. Poulakakis are with the Department of Mechanical Engineering, University of Delaware, Newark, DE 19716, USA; e-mail: {xinliu, poulakas}@udel.edu.

This work is supported in part by by NSF grant CMMI-1130372 and ARO contract W911NF-12-1-0117

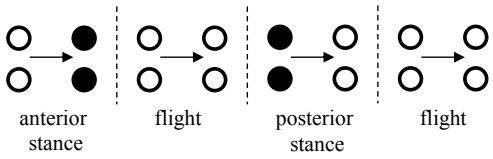

Fig. 2. Footfall pattern of a nominal bounding gait; solid circles indicate legs in contact with the ground and white circles indicate legs in the air.

the stance-posterior "sp" and the flight "f" phases. These phases are separated by touchdown and liftoff events, which are denoted by "td" and "lo," respectively.

TABLE I

MECHANICAL PARAMETERS OF THE MODEL

Parameter	Value	Units
Torso Mass (m)	20.865	kg
Torso Inertia (J)	1.39	kg m^2
Hip-to-COM spacing (L)	0.276	m
Nominal Leg Length (l_0)	0.323	m
Leg Spring Constant (k_{leg})	7040	N/m

A. Dynamics in Continuous Time

In each phase, the configuration space Q is a simply-connected open subset of $\mathbb{R}^2 \times \mathbb{S}^1$, and can be parameterized by the Cartesian coordinates x_{cm} and y_{cm} of the COM together with the torso angle θ, i.e., $q = (x_{\mathrm{cm}}, y_{\mathrm{cm}}, \theta)' \in Q$. For each $i \in \{\mathrm{sa}, \mathrm{f}, \mathrm{sp}\}$, the dynamics can be written in state-space form as

$$\dot{x} = f_i(x), \tag{1}$$

where $x \in \mathcal{X} := \{(q', \dot{q}')' \mid q \in Q,\ \dot{q} \in \mathbb{R}^3\}$.

B. Event-based Transition

Transitions between different phases occur when certain threshold functions $H : \mathcal{X} \to \mathbb{R}$ cross zero. Assuming that liftoff occurs when a leg reaches its natural length as it extends, the threshold functions that correspond to the anterior and posterior legs liftoff are, respectively,

$$H_{\mathrm{sa}\to\mathrm{f}}(x) = l_0 - \sqrt{(x_{\mathrm{cm}} + L\cos\theta)^2 + (y_{\mathrm{cm}} + L\sin\theta)^2} \tag{2}$$

$$H_{\mathrm{sp}\to\mathrm{f}}(x) = l_0 - \sqrt{(x_{\mathrm{cm}} - L\cos\theta)^2 + (y_{\mathrm{cm}} - L\sin\theta)^2} \tag{3}$$

where l_0 is the natural (uncompressed) leg length. On the other hand, the threshold functions that describe touchdown events are defined as

$$H_{\mathrm{f}\to\mathrm{sp}}(x, \gamma_{\mathrm{p}}) = y_{\mathrm{cm}} - L\sin\theta - l_0\cos\gamma_{\mathrm{p}} \tag{4}$$

$$H_{\mathrm{f}\to\mathrm{sa}}(x, \gamma_{\mathrm{a}}) = y_{\mathrm{cm}} + L\sin\theta - l_0\cos\gamma_{\mathrm{a}} \tag{5}$$

corresponding to toe height. Notice that γ_{p} and γ_{a} in (4) and (5) are parameters available for control, and can be selected through a leg angle control policy.

C. Flow, Flow Maps and Poincaré Return Map

For each $i \in \{\mathrm{sa}, \mathrm{f}, \mathrm{sp}\}$, let $\hat{\phi}_i(t, x_0)$, $t \geq t_0$, be a maximal solution of (1) with initial condition $x_0 \in TQ$; that is, $\hat{\phi}_i(t_0, x_0) = x_0$ and

$$\hat{\phi}_i(t, x_0) = x_0 + \int_{t_0}^{t} f_i\left(\hat{\phi}_i(\tau, x_0)\right) d\tau \ . \tag{6}$$

With a slight abuse of notation, define $\hat{\phi}_i^t(x_0) = \hat{\phi}_i(t, x_0)$. The continuous time evolution of the system is interrupted when the corresponding threshold function becomes zero. The time-to-switch function $T_i : \mathcal{X} \to \mathbb{R}$ for each phase $i \in \{\mathrm{sa}, \mathrm{f}, \mathrm{sp}\}$ is defined by

$$T_{\mathrm{sa}}(x_0) = \inf\{t > 0 \mid H_{\mathrm{sa}\to\mathrm{f}}(\hat{\phi}_{\mathrm{sa}}^t(x_0)) = 0\} \tag{7}$$

$$T_{\mathrm{sp}}(x_0) = \inf\{t > 0 \mid H_{\mathrm{sp}\to\mathrm{f}}(\hat{\phi}_{\mathrm{sp}}^t(x_0)) = 0\} \tag{8}$$

$$T_{\mathrm{f}}(x_0, \gamma) = \inf\{t \geq 0 \mid H_{\mathrm{f}\to\mathrm{sa}\ \text{or}\ \mathrm{f}\to\mathrm{sp}}(\hat{\phi}_{\mathrm{f}}^t(x_0), \gamma) = 0\}, \tag{9}$$

where $\gamma \in \{\gamma_{\mathrm{p}}, \gamma_{\mathrm{a}}\}$. With these definitions at hand, the flow map $\hat{F}_i : \mathcal{X} \to \mathcal{X}$ for each phase $i \in \{\mathrm{sa}, \mathrm{f}, \mathrm{sp}\}$ is

$$\hat{F}_i(x_0) = \hat{\phi}_i^{T_i(x_0)}(x_0) \ . \tag{10}$$

In words, the flow map takes "entry" conditions to "exit" conditions for each phase. Assume, without loss of generality, that the bounding cycle begins at the touchdown of the anterior leg, and let $\mathcal{S}_{\mathrm{sa}} \subset \mathcal{X}$ be the set of anterior leg touchdown states that result in the completion of a stride. The stride map $\hat{F} : \mathcal{S}_{\mathrm{sa}} \to \mathcal{X}$ can then be defined through the composition of the corresponding flow maps as

$$\hat{F} = \hat{F}_{\mathrm{f}} \circ \hat{F}_{\mathrm{sp}} \circ \hat{F}_{\mathrm{f}} \circ \hat{F}_{\mathrm{sa}} \ . \tag{11}$$

To evaluate stability, the method of Poincaré is used. Since the horizontal position x_{cm} of the COM is a monotonically increasing cyclic variable, it will be projected out from the stride map. Let Π be the projection of the state vector x to its non-x_{cm} component $z = (y_{\mathrm{cm}}, \theta, \dot{x}_{\mathrm{cm}}, \dot{y}_{\mathrm{cm}}, \dot{\theta})'$

$$\Pi(x) := \begin{bmatrix} 0 & \mathbf{0}_{1\times 5} \\ \mathbf{0}_{5\times 1} & I_{5\times 5} \end{bmatrix} x \tag{12}$$

and define the maps

$$\Sigma_{\mathrm{sa}}(z) := \begin{pmatrix} -L\cos\theta - \sqrt{l_0^2 - (y_{\mathrm{cm}} + L\sin\theta)^2} \\ z \end{pmatrix} \tag{13}$$

$$\Sigma_{\mathrm{sp}}(z) := \begin{pmatrix} L\cos\theta - \sqrt{l_0^2 - (y_{\mathrm{cm}} - L\sin\theta)^2} \\ z \end{pmatrix} \tag{14}$$

which recover the horizontal position of the COM with respect to a local frame attached at the toe of the support leg. Then, the Poincaré return map $P : \Pi(\mathcal{S}_{\mathrm{sa}}) \to \Pi(\mathcal{S}_{\mathrm{sa}})$ can be defined through the stride map (11) as

$$\begin{aligned} P &= \Pi \circ \hat{F} \circ \Sigma_{\mathrm{sa}} \\ &= \Pi \circ \hat{F}_{\mathrm{f}} \circ \hat{F}_{\mathrm{sp}} \circ (\Sigma_{\mathrm{sp}} \circ \Pi) \circ \hat{F}_{\mathrm{f}} \circ \hat{F}_{\mathrm{sa}} \circ \Sigma_{\mathrm{sa}} \\ &= F_{\mathrm{f}} \circ \Pi \circ \hat{F}_{\mathrm{sp}} \circ \Sigma_{\mathrm{sp}} \circ F_{\mathrm{f}} \circ \Pi \circ \hat{F}_{\mathrm{sa}} \circ \Sigma_{\mathrm{sa}} \\ &= F_{\mathrm{f}} \circ F_{\mathrm{sp}} \circ F_{\mathrm{f}} \circ F_{\mathrm{sa}} \ , \end{aligned} \tag{15}$$

where F_{f} is the restriction of $\hat{F}_{\mathrm{f}}$ on $\Pi(\mathcal{X})$ so that $\Pi \circ \hat{F}_{\mathrm{f}} = F_{\mathrm{f}} \circ \Pi$ due to the decoupling of the horizontal motion from the vertical and the rotational motions during flight, and $F_i := \Pi \circ \hat{F}_i \circ \Sigma_i$, $i \in \{\mathrm{sa}, \mathrm{sp}\}$. Note that the first equality in (15) is due to the fact that $\Sigma_{\mathrm{sp}} \circ \Pi = \mathrm{id}$ on the range of $\hat{F}_{\mathrm{f}} \circ \hat{F}_{\mathrm{sa}} \circ \Sigma_{\mathrm{sa}}$.

D. Passive Periodic Bounding Gaits

A number of fixed points of the Poincaré return map (15) that correspond to bounding motions can be found numerically. It has been observed that these motions satisfy certain symmetry conditions that will be important in the analysis of the following section; see [8] for a detailed discussion. Figure 3 presents the state evolution for one such fixed point $\bar{z}$. Focusing on the stance phases, it can be seen that the evolution forward in time of the anterior stance phase based on the corresponding initial condition $\bar{x}_{\rm sa} = \Sigma_{\rm sa}(\bar{z})$ is indistinguishable from the evolution of the posterior stance phase traversed *backward* in time based on the initial condition $\bar{x}_{\rm sp} = \hat{G} \cdot \bar{x}_{\rm sa}$, where $\hat{G} = \mathrm{diag}\,[-1, 1, -1, 1, -1, 1]$. Furthermore, if we define $G := \mathrm{diag}\,[1, -1, 1, -1, 1]$, then

$$G \circ F_{\rm sp} \circ F_{\rm f} \circ F_{\rm sa}(\bar{z}) = \bar{z} \ . \tag{16}$$

Finally, as was observed in [8], fixed points satisfy the property that the touchdown angle of the posterior (anterior) leg is equal to the negative of the liftoff value of the anterior (posterior) leg; i.e., $\gamma_{\rm a}^{\rm td} = -\gamma_{\rm p}^{\rm lo}$ and $\gamma_{\rm p}^{\rm td} = -\gamma_{\rm a}^{\rm lo}$. Note that this property is similar to that observe in the SLIP [4], [6]. Bounding gaits that enjoy such symmetry properties are at the center of this work, the purpose of which is to analyze the stability of these motions by exploiting the symmetries of the underlying vector fields.

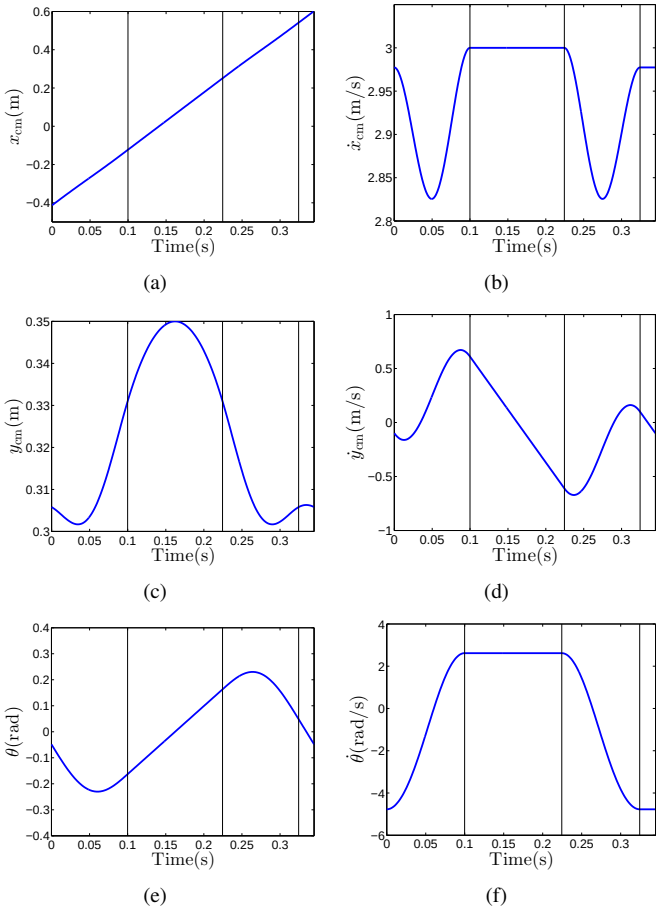

Fig. 3. State evolution at a symmetric bounding gait starting at anterior leg touchdown. Vertical lines represent subsequent events; from left to right: anterior leg liftoff, posterior leg touchdown, posterior leg liftoff.

III. Necessary Conditions for Stability

For periodic bounding gaits, a common approach to evaluate stability is by *numerically* computing the eigenvalues of the linearization of the Poincaré map about a fixed point [8]. In contrast, this paper uses the framework introduced in [4] to state *analytical* expressions that are necessary for stability (and sufficient for instability).

A. Basic Concepts

Consider the discrete map P and let $\bar{z}$ be a fixed point of P; that is, $P(\bar{z}) = \bar{z}$. If $\bar{z}$ were an asymptotically stable fixed point and z_0 were in the domain of attraction of $\bar{z}$, then $\lim_{k\to\infty} P^k(z_0) = \bar{z}$, where $P^k = P \circ \cdots \circ P$. This observation implies that locally, in a neighborhood of an asymptotically stable fixed point, the volume of P shrinks; mathematically,

$$|\det(D_z P(\bar{z}))| < 1 \ , \tag{17}$$

which provides a condition that is *necessary* for stability [4]. However, (17) is *not* sufficient[1]; in fact, we will be concerned with fixed points $\bar{z}$ of P defined by (15) that satisfy (17) and are not asymptotically stable; for, perturbations that shift the total energy of the system cannot be rejected in the conservative setting of the model[2]. Nevertheless, (17) provides important information for selecting control parameters, due to the fact that $\det(D_z P(\bar{z}))$ can be computed analytically in a neighborhood of a fixed point.

The computation of $\det(D_z P(\bar{z}))$ in (17) can be facilitated if the vector fields underlying the construction of P satisfy certain symmetry properties. In particular, the notion of time-reversal symmetries of vector fields is the additional structure we require. Let f be a vector field defined on a chart $\mathcal{X}$, and consider the dynamical system $\dot{x} = f(x)$. A diffeomorphism $G : \mathcal{X} \to \mathcal{X}$ is a time-reversal symmetry, if

$$D_x G \cdot f = -f \circ G \ , \tag{18}$$

where $D_x G$ denotes the derivative of G in x. Equivalently, in terms of the flow ϕ^t associated with $\dot{x} = f(x)$,

$$G \circ \phi^t = \phi^{-t} \circ G \ . \tag{19}$$

Time reversal symmetries have been employed to study conservative reductive models of legged locomotion in [4] under the additional assumption of involutivity; that is,

$$G \circ G = \mathrm{id}_{\mathcal{X}} \ , \tag{20}$$

where $\mathrm{id}_{\mathcal{X}}$ is the identity map on $\mathcal{X}$. The framework introduced in [4] is suitable for analyzing periodic orbits of systems, in which the Poincaré map P can be written as the composition of time-reversed flow maps $P_\alpha = G_\alpha \circ F_\alpha$, i.e.

$$P = P_1 \circ \cdots \circ P_n \Rightarrow P = (G_1 \circ F_1) \circ \cdots \circ (G_n \circ F_n) \tag{21}$$

[1]For sufficient conditions of stability, all the eigenvalues of the linearization of the Poincaré map are needed, not just their product that is equal to the determinant in (17).

[2]In Section IV-B below we will introduce non-conservative control inputs at the hip joint and a controller that regulates the total energy of the system to achieve asymptotic stabilization.

where F_α is the flow map of a vector field f_α, i.e., $F_\alpha(x) := \phi_\alpha^{T_\alpha(x)}(x)$ and G_α is an involutive time-reversal symmetry for $\alpha \in \{1, ..., n\}$. In general, if a map P_α is involutive, the following theorem proved in [4] simplifies the computation of the determinant of its Jacobian at a fixed point.

Theorem 1 ([4, Theorem 3]): Let $\bar{z} \in \mathcal{S}$ be a fixed point of a map $P_\alpha : \mathcal{S} \to \mathcal{S}$, where $\mathcal{S}$ contains a neighborhood of $\bar{z}$. If P_α is an involution, the determinant of its Jacobian $D_z P_\alpha$ evaluated at $\bar{z}$ is $|\det(D_z P_\alpha(\bar{z}))| = 1$.

The significance of the decomposition (21) lies in the case that a fixed point $\bar{z}$ of the overall Poincaré map P is also a fixed point of *all* the factors P_α, i.e.,

$$\bar{z} = P(\bar{z}) \Rightarrow \bar{z} = (G_\alpha \circ F_\alpha)(\bar{z}) \tag{22}$$

for $\alpha \in \{1, ..., n\}$. Then, if any of the constituent maps $P_\alpha = G_\alpha \circ F_\alpha$ is an involution, the finite volume preservation property established by Theorem 1 can be used to facilitate the computation of the determinant of the linearization of the overall Poincaré map at a fixed point. As a result, analytical conditions that are necessary for stability can be stated through the use of (17).

It turns out that for a class of important locomotion models that includes the Spring Loaded Inverted Pendulum (SLIP), the condition (22) is satisfied naturally. For example, in the SLIP implementing a hopping gait, a fixed point of the Poincaré map is also a fixed point of the flight and stance time-reversed flow maps [4]. However, in the case of bounding gaits, insisting that a fixed point of the Poincaré map is also a fixed point of the stance-posterior, flight and stance-anterior phases would be rather restrictive and would result in unnatural bounding motions. The following section proposes a *controlled* factorization of the Poincaré map, which, under a simple leg placement policy, allows us to circumvent this issue.

B. Main Result: Necessary Conditions for Stability

The Poincaré map in (15) can be factored as

$$P = \underbrace{F_{\mathrm{f}} \circ G}_{P_2} \circ \underbrace{G \circ F_{\mathrm{sp}} \circ F_{\mathrm{f}} \circ F_{\mathrm{sa}}}_{P_1} \ , \tag{23}$$

where $G = \mathrm{diag}\ [1, -1, 1, -1, 1]$ and $G \cdot G = I_{5\times 5}$ the identity matrix. Note that P_1 in (23) does *not* correspond to the time-reversed flow map of an individual phase; rather it is the time-reversed composition of three flow maps.

We begin with Theorem 2, which establishes conditions under which, P_1 is an involution; that is,

$$(G \circ F_{\mathrm{sp}} \circ F_{\mathrm{f}} \circ F_{\mathrm{sa}}) \circ (G \circ F_{\mathrm{sp}} \circ F_{\mathrm{f}} \circ F_{\mathrm{sa}}) = \mathrm{id}_{\Pi(\mathcal{S}_{\mathrm{sa}})}. \tag{24}$$

Theorem 2: Let $\gamma_{\mathrm{a}}^{\mathrm{td}}$ be the touchdown angle of the anterior leg. Define $\mathcal{S}_{\mathrm{sa}} := \{x \in \mathcal{X} \mid H_{\mathrm{f}\to\mathrm{sa}}(x, \gamma_{\mathrm{a}}^{\mathrm{td}}) = 0, \dot{y}_{\mathrm{cm}} < 0, \dot{\theta} < 0\}$ and let $\Pi(\mathcal{S}_{\mathrm{sa}})$ be the projection as per (12). If

$$\gamma_{\mathrm{p}}^{\mathrm{td}} = -\gamma_{\mathrm{a}}^{\mathrm{lo}} \ , \tag{25}$$

then, P_1 is an involution on $\Pi(\mathcal{S}_{\mathrm{sa}})$. Furthermore, if $\bar{z} \in \Pi(\mathcal{S}_{\mathrm{sa}})$ is a fixed point of P shared by P_1, we have that $|\det(D_z P_1)(\bar{z}))| = 1$.

The proof of Theorem 2 is organized in two lemmas. The first shows that the flow maps F_{sa} and F_{sp} are G-related.

Lemma 1: Let $\mathcal{S}_{\mathrm{sp}}$ and $\mathcal{S}_{\mathrm{sa}}$ be the sets of posterior and anterior touchdown states that result in the completion of a stride, respectively. Then,

(i) $F_{\mathrm{sa}} \circ G \circ F_{\mathrm{sp}} = G$, on $\Pi(\mathcal{S}_{\mathrm{sp}})$,
(ii) $F_{\mathrm{sp}} \circ G \circ F_{\mathrm{sa}} = G$, on $\Pi(\mathcal{S}_{\mathrm{sa}})$,

where Π denotes the projection map defined by (12).

Proof: We begin with statement (i). By inspecting f_{sa} and f_{sp} it can be verified directly that $\hat{G} \circ f_{\mathrm{sp}} = -f_{\mathrm{sa}} \circ \hat{G}$, where $\hat{G} = \mathrm{diag}\ [-1, 1, -1, 1, -1, 1]$ and $\hat{G} \cdot \hat{G} = I_{6\times 6}$. Integrating based on an initial condition $x_0 \in \mathcal{S}_{\mathrm{sp}}$ results in

$$\hat{G} \circ \hat{\phi}_{\mathrm{sp}}^{t} = \hat{\phi}_{\mathrm{sa}}^{-t} \circ \hat{G} \ . \tag{26}$$

Next we show that $T_{\mathrm{sp}}(x_0) = T_{\mathrm{sa}}(\hat{G}(x_0))$. According to (26), $H_{\mathrm{sp}\to\mathrm{f}} \circ \hat{\phi}_{\mathrm{sp}}^{t} = H_{\mathrm{sp}\to\mathrm{f}} \circ \hat{G} \circ \hat{\phi}_{\mathrm{sa}}^{-t} \circ \hat{G}$. Now, by the definitions (2) and (3) of the corresponding threshold functions observe that $H_{\mathrm{sp}\to\mathrm{f}} = H_{\mathrm{sa}\to\mathrm{f}} \circ \hat{G}$. Then, $H_{\mathrm{sp}\to\mathrm{f}} \circ \hat{G} \circ \hat{\phi}_{\mathrm{sa}}^{-t} \circ \hat{G} = H_{\mathrm{sa}\to\mathrm{f}} \circ \hat{\phi}_{\mathrm{sa}}^{-t} \circ \hat{G}$, and hence

$$H_{\mathrm{sp}\to\mathrm{f}} \circ \hat{\phi}_{\mathrm{sp}}^{t} = H_{\mathrm{sa}\to\mathrm{f}} \circ \hat{\phi}_{\mathrm{sa}}^{-t} \circ \hat{G}. \tag{27}$$

This implies that the value of $H_{\mathrm{sp}\to\mathrm{f}}$ along the flow $\hat{\phi}_{\mathrm{sp}}^{t}(x_0)$ is equal to the value of $H_{\mathrm{sa}\to\mathrm{f}}$ along the time-reversed flow $\hat{\phi}_{\mathrm{sa}}^{-t} \circ \hat{G}(x_0)$. Since by (7) and (8), T_{sp} and T_{sa} represent the minimal solutions of the corresponding threshold equations being equal to zero, (27) implies $T_{\mathrm{sp}}(x_0) = T_{\mathrm{sa}}(\hat{G}(x_0))$. Applying the projection map Π (12) completes the proof. Statement (ii) can be shown using similar arguments. ■

Remark 1: Figure 4 provides some intuition on Lemma 1. Due to the fact the vector fields f_{sp} and f_{sa} of the stance-posterior and stance-anterior phases are related through $\hat{G}$, the evolution of the stance-posterior phase starting from initial conditions $z_A = \Pi(x_A)$ and progressing forward in time is *indistinguishable* from the evolution of the stance-anterior phase starting from the corresponding *G-reflected* initial conditions, $z_D = \Pi(\hat{G}x_A) = Gz_A$, and progressing *backward* in time. Lemma 1 establishes that not only the flows, but also the flow maps of the two phases are G-related due to the fact that the corresponding threshold functions "preserve" the time reversal symmetry G.

Next we show that the flow map of the flight phase prior to the posterior-stance is G-related with the flow map of the flight phase prior to the anterior-stance phase, *provided* that the touchdown angle of the posterior leg is selected according to the simple control law (25).

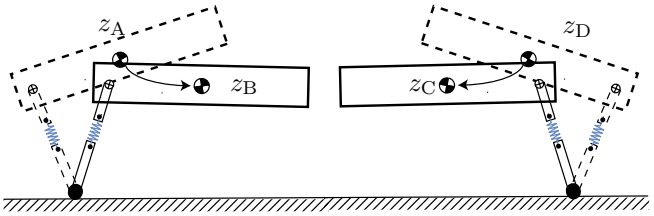

Fig. 4. The stance-posterior and stance-anterior phases are related through a time-reversal symmetry.

Lemma 2: Let $\gamma_{\rm a}^{\rm lo}$ be the anterior leg liftoff angle. Define $\mathcal{S}_{\rm f} := \{x \in \mathcal{X} \mid H_{\rm sa\to f}(x) = 0, \dot{y}_{\rm cm} > 0\}$ and let $\Pi(\mathcal{S}_{\rm f})$ be the projection as per (12). If the posterior leg touchdown angle is selected according to (25), then $F_{\rm f} \circ G \circ F_{\rm f} = G$.

Proof: (sketch) The condition $\gamma_{\rm p}^{\rm td} = -\gamma_{\rm a}^{\rm lo}$ guarantees that the time-to-switch functions for the two phases satisfy $T_{\rm f}(x_0) = T_{\rm f}(\hat{G}(x_0))$. The arguments are identical to those in the proof of Lemma 1 and are omitted for brevity. ■

The proof of Theorem 2 is provided next.

Proof: [Theorem 2] The proof is an immediate consequence of Theorem 1 in view of the Lemmas 1 and 2. ■

With Theorem 2 in hand, we can now state necessary conditions for the stability of a periodic bounding gait. The determinant of the Poincaré map at a fixed point $\bar{z}$ realized under the touchdown angle control policy suggested by Theorem 2 can be computed as

$$\begin{aligned}|\det(D_z P(\bar{z}))| &= |\det(D_z P_2(P_1(\bar{z}))) \cdot \det(D_z P_1(\bar{z}))| \\ &= |\det(D_z P_2(\bar{z}))| = |\det(D_z F_{\rm f}(\bar{z}))|.\end{aligned}$$

A necessary condition for $\bar{z}$ to be a stable fixed point of P is $|\det(D_z F_{\rm f}(\bar{z}))| < 1$. Note that $F_{\rm f}$ is the flow map of the flight following the posterior stance and that the corresponding touchdown angle has not been fixed by the procedure, thus it is available for control.

Given an initial condition $z_0 = \Pi(x_0)$, the fight phase flow map $F_{\rm f}$ can be computed analytically due to the integrability of the underlying vector field $f_{\rm f}$; i.e.,

$$F_{\rm f}(z_0) = \begin{pmatrix} y_{\rm cm,0} + \dot{y}_{\rm cm,0} T_{\rm f} - \frac{1}{2} g T_{\rm f}^2 \\ \theta_0 + \dot{\theta}_0 T_{\rm f} \\ \dot{x}_{\rm cm,0} \\ \dot{y}_{\rm cm,0} - g T_{\rm f} \\ \dot{\theta}_0 \end{pmatrix} \tag{28}$$

where[3] $T_{\rm f} = T_{\rm f}(z_0, \gamma_{\rm a})$ is an implicit function of initial state and front leg angle, which will be determined by a feedback law of the form $\gamma_{\rm a}(z_0)$. $T_{\rm f}$ can be described by zeroing the threshold equation $H_{\rm f\to sa}$:

$$y_{\rm cm} + \dot{y}_{\rm cm} T_{\rm f} - \frac{g T_{\rm f}^2}{2} + L\sin(\theta_0 + \dot{\theta} T_{\rm f}) - l_0 \cos\gamma_{\rm a}^{\rm td} = 0 \tag{29}$$

The determinant of $D_z F_{\rm f}(z_0)$ can be computed by

$$\det(D_z F_{\rm f}) = 1 - g\frac{\partial T_{\rm f}}{\partial \dot{y}_{\rm cm,0}} + \dot{y}_{\rm cm,0}\frac{\partial T_{\rm f}}{\partial y_{\rm cm,0}} + \dot{\theta}_0 \frac{\partial T_{\rm f}}{\partial \theta_0} \tag{30}$$

The partial derivative of $T_{\rm f}$ in the determinant can be replaced using implicit differentiation rules on (29). After some manipulation, $D_z F_{\rm f}(z_0)$ can be written as

$$\det(D_z F_{\rm f}(z_0)) = \frac{\Delta_1}{-\Delta_2} \ , \tag{31}$$

where

$$\Delta_1 = \sin\gamma_{\rm a} l_0 \left(\dot{y}_{\rm cm,0}\frac{\partial \gamma_{\rm a}^{\rm td}}{\partial y_{\rm cm,0}} + \dot{\theta}_0 \frac{\partial \gamma_{\rm a}^{\rm td}}{\partial \theta_0} - g\frac{\partial \gamma_{\rm a}^{\rm td}}{\partial \dot{y}_{\rm cm,0}} - \frac{\partial \gamma_{\rm a}^{\rm td}}{\partial T_{\rm f}} \right)$$

$$\Delta_2 = \dot{y}_{\rm cm,0} - g T_{\rm f} + \dot{\theta}_0 L\cos(\theta_0 + \dot{\theta}_0 T_{\rm f}) + l_0 \sin\gamma_{\rm a}^{\rm td}\frac{\partial \gamma_{\rm a}^{\rm td}}{\partial T_{\rm f}}$$

[3]By (5), $H_{\rm f\to sa}$ does not depend on $x_{\rm cm}$, thus $T_{\rm f}$ is a function of z.

IV. Controller Design For Bounding Gaits

Based on the analysis in Section III, a controller is derived first that ensures convergence to a fixed point in the presence of perturbations that do not alter the energy level of the system. To reject perturbations that alter the total energy, actuation will be introduced at the hip joints during stance to regulate the energy of the system at a desired level.

A. Stabilization within a Constant Energy Level

Based on the condition (25) of Theorem 2, we set

$$\gamma_{\rm p}^{\rm td}[n] = -\gamma_{\rm a}^{\rm lo}[n] \ , \tag{32}$$

and we employ the following feedback controller to regulate the touchdown angle of the anterior leg

$$\gamma_{\rm a}^{\rm td}[n] = \bar{\gamma}_{\rm a}^{\rm td} + c(\bar{\gamma}_{\rm p}^{\rm lo} - \gamma_{\rm p}^{\rm lo}[n]) \tag{33}$$

where $\bar{\gamma}_{\rm a}^{\rm td}$ and $\bar{\gamma}_{\rm p}^{\rm lo}$ are the anterior leg liftoff and the posterior leg touchdown angles at a fixed point; c is a constant gain, and $\gamma_{\rm p}^{\rm lo}$ is the posterior leg's liftoff angle.

Noticing that $\gamma_{\rm p}^{\rm lo} = -\text{acos}(\frac{y_{\rm cm,0} - L\sin\theta_0}{l_0})$ and using $\gamma_{\rm p}^{\rm td} = -\gamma_{\rm a}^{\rm lo}$ at a symmetric fixed point $\bar{z}_0$, the determinant of the Jacobian of the Poincaré return map at fixed point $\bar{z}$ is

$$|\det(D_z P(\bar{z}))| = |\det(D_z F_{\rm f}(\bar{z}))| = |c|. \tag{34}$$

As a result, based on our previous analysis, a necessary condition for the system to be stable is $c \in (-1, 1)$.

Fig. 5 shows the discrete evolution of the system in closed loop with the controller (32)-(33) under a perturbation away from the fixed point of Fig. 3. The perturbation does not change the total energy of the system. Three different values of c are considered. Although, (34) is necessary but not sufficient for stability, it can be seen that for $c = 0.5 < 1$ the system converges to a fixed point. For $c = 1$ the evolution oscillates around the fixed point while it diverges for $c > 1$. Finally, to fully characterize stability, Fig. 6 presents the root locus of the eigenvalues of the linearization of the Poincaré map for different values of c at the fixed point. It can be seen that for $|c| > 1$ the system is indeed unstable.

B. Asymptotic Stabilization of a Bounding Gait

Conservation of energy in the model of Fig. 1 precludes asymptotically stable fixed points; for, perturbations altering the total energy of the system cannot be rejected. A simple controller is proposed here that is capable of asymptotically stabilizing bounding motions of the system.

1) Energy Controller: To regulate the system's energy, two actuators are introduced at the hip joints of the posterior and the anterior legs. Each actuator acts only when the corresponding leg is on the ground, and deliver torques computed according to the prescription

$$\tau = -K \ \frac{E - \bar{E}}{\Delta\bar{\varphi}}, \tag{35}$$

where $\Delta\bar{\varphi}$ is a constant, corresponding to the change of the stance leg angle φ relative to the torso at the fixed point; E is the total energy and $\bar{E}$ is the nominal value at the fixed point, and $K \in [0, 1]$, controls the converging rate.

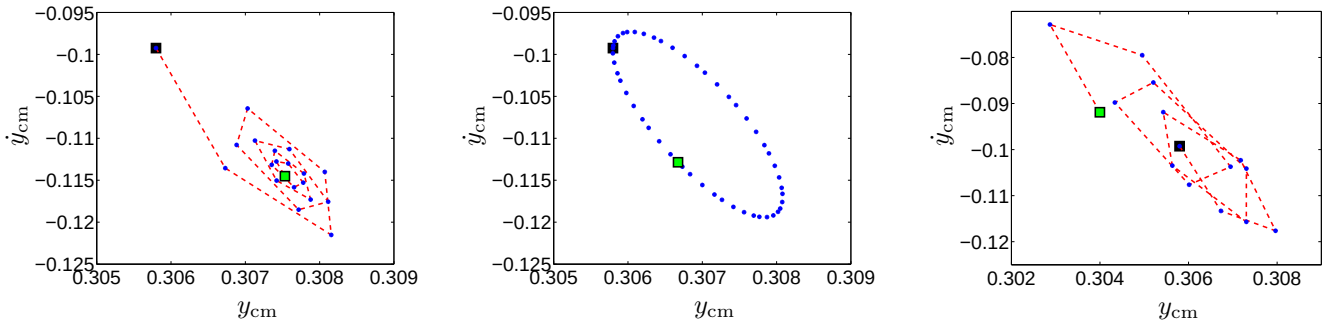

(a) (b) (c)

Fig. 5. Discrete evolution of the closed loop system (blue dots) under a perturbation that leaves the system's total energy unchanged. The initial state is marked by the black square while the final condition is marked as green square. 5(a): $c = 0.5$; 5(b): $c = 1$; and 5(c): $c = 1.2$.

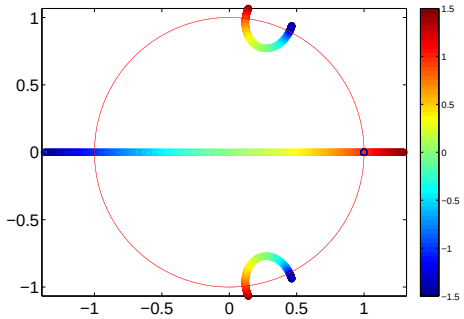

Fig. 6. Locus of the eigenvalues as c varies in $[-1.5, 1.5]$.

2) Velocity Feedback: To prevent the system from converging to a nearby fixed point within the same energy level, the posterior leg touchdown angle controller (32) is modified to include a "symmetry-breaking" term, as follows

$$\gamma_{\rm p}^{\rm td}[n] = -\gamma_{\rm a}^{\rm lo}[n] + K_{\rm vel}(\bar{\dot{x}}_{\rm cm} - \dot{x}_{\rm cm}) \ , \qquad (36)$$

where $K_{\rm vel}$ is a gain multiplying the error between the nominal (fixed point) $\bar{\dot{x}}_{\rm cm}$ and the current $\dot{x}_{\rm cm}$ velocity.

3) Simulation Results: Fig. 7 presents the performance of the controller under control laws (33), (35) and (36). The control coefficients are chosen as $c = 0.1$, $K = 0.1$ and $K_{\rm vel} = 0.05$. Linearization of the Poincaré return map gives a dominant eigenvalue of 0.89, suggesting that the fixed point is locally exponentially stable.

V. Conclusion

This paper analyzed stability of passive bounding gaits based on a reductive sagittal-plane model. For conservative piecewise holonomic systems, the approach used here offers *analytically expressed* necessary conditions for stability.

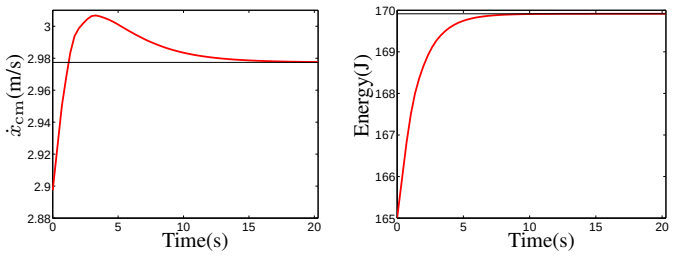

(a) (b)

Fig. 7. Evolution of the horizontal velocity (a) and total energy (b) at anterior touchdown in response to a $0.08{\rm m/s}$ disturbance in $\dot{x}_{\rm cm}$; black lines correspond to nominal values.

Inspired by this analysis, a simple touchdown angle policy is devised with its control gains so that the necessary condition for stability is satisfied. The control policy is further augmented with an energy controller and velocity feedback to asymptotically stabilize periodic bounding gaits. The performance of the controller is evaluated by simulation.

References

[1] P. Holmes, R. J. Full, D. Koditschek, and J. Guckenheimer, "The dynamics of legged locomotion: Models, analyses, and challenges," *SIAM Review*, vol. 48, no. 2, pp. 207–304, May 2006.

[2] M. Raibert, "Symmetry in running," *Science*, vol. 231, no. 4743, pp. 1292–1294, 1986.

[3] M. H. Raibert, *Legged Robots that Balance*. Cambridge, MA: MIT Press, 1986.

[4] R. Altendorfer, D. E. Koditschek, and P. Holmes, "Stability analysis of legged locomotion models by symmetry-factored return maps," *The International Journal of Robotics Research*, vol. 23, no. 10-11, pp. 979–999, Oct. 2004.

[5] J. Lamb and J. Roberts, "Time-reversal symmetry in dynamical systems: A survey," *Physica D: Nonlinear Phenomena*, vol. 112, no. 1-2, pp. 1–39, 1998.

[6] W. J. Schwind, "Spring loaded inverted pendulum running: A plant model," Ph.D. dissertation, University of Michigan, 1998.

[7] R. Altendorfer, D. E. Koditschek, and P. Holmes, "Stability analysis of a clock-driven rigid-body SLIP model for RHex," *The International Journal of Robotics Research*, vol. 25, no. 4, pp. 343–358, 2006.

[8] I. Poulakakis, E. Papadopoulos, and M. Buehler, "On the stability of the passive dynamics of quadrupedal running with a bounding gait," *The International Journal of Robotics Research*, vol. 25, no. 7, pp. 669–687, 2006.

[9] Z. Zhang, Y. Fukuoka, and H. Kimura, "Stable quadrupedal running based spring-loaded two-segment legged on a model," in *Proceedings of IEEE International Conference on Robotics and Automation*, vol. 3, 2004, pp. 2601–2606.

[10] P. Chatzakos and E. Papadopoulos, "Self-stabilising quadrupedal running by mechanical design," *Applied Bionics and Biomechanics*, vol. 6, no. 1, pp. 73–85, 2009.

[11] Z. G. Zhang, H. Kimura, and Y. Fukuoka, "Autonomously generating efficient running of a quadruped robot using delayed feedback control," *Advanced Robotics*, vol. 20, no. 6, pp. 607–629, 2006.

[12] Z. G. Zhang, T. Masuda, H. Kimura, and K. Takase, "Towards realization of adaptive running of a quadruped robot using delayed feedback control," in *Proceedings of IEEE International Conference on Robotics and Automation*, 2007, pp. 4325–4330.

[13] Y. Fukuoka, H. Kimura, and A. H. Cohen, "Adaptive dynamic walking of a quadruped robot on irregular terrain based on biological concepts," *The International Journal of Robotics Research*, vol. 22, no. 3-4, pp. 187–202, 2003.

[14] A. K. Valenzuela and S. Kim, "Optimally scaled hip-force planning: A control approach for quadrupedal running,," in *Proceedings of IEEE International Conference on Robotics and Automation*, Minnesota, USA, May 2012, pp. 1901–1907.